RSC Advances

PAPER

View Article Online
View Journal | View Issue

Cite this: *RSC Adv.*, 2015, **5**, 1438

Performance comparison of two cascade reaction models in fluorescence off–on detection of hydrogen sulfide†

Tanmoy Saha, Dnyaneshwar Kand and Pinaki Talukdar*

Received 24th October 2014
Accepted 24th November 2014

DOI: 10.1039/c4ra13086c

www.rsc.org/advances

Comparative studies on the performances of two cascade reaction based fluorescent H_2S probes are reported. These probes were also designed to address the solubility issues of existing probes. The **Reso-N_3** probe favors the H_2S mediated azide-to-amine reduction followed by a cyclization to release the resorufin fluorophore. **Reso-Br** undergoes a bromide-to-thiol nucleophilic substitution followed by a similar cyclization releasing the same fluorophore. **Reso-N_3** exhibited lower background fluorescence and better H_2S sensing behavior in water compared to **Reso-Br**. **Reso-Br** underwent hydrolysis in aqueous buffer conditions (pH = 7.4) while, **Reso-N_3** was quite stable. **Reso-N_3** displayed high selectivity and sensitivity towards H_2S. Live cell imaging of the species by the probe was also established.

Introduction

Hydrogen sulfide (H_2S) is a colorless, toxic, inflammable, corrosive gas, and it is produced mainly from geological and microbial activities.[1,2] The species has a characteristic smell of rotten eggs and its detectability threshold by a healthy human nose ranges from 0.005–0.3 ppm. This gaseous species when exposed or inhaled in excess, can cause respiratory failure, loss of consciousness, sudden cardiac death, hepatic[2] and olfactory paralysis. Endogenously, H_2S can be produced during metabolism of cysteine (Cys) catalyzed by two pyridoxal 5′-phosphate dependent enzymes *i.e.* cystathionine-β-synthase (CBS),[3] and cystathionine-γ-layse (CSE)[4] and one pyridoxal 5′-phosphate independent enzyme *i.e.* 3-Mercaptopyruvate sulfurtransferase (3-MST).[5] 3-MST is a mitochondrial and cytosolic enzyme (found in brain tissues)[6] whereas CBS and CSE are exclusively cytosolic (found in liver and brain tissues). Although, H_2S has been viewed primarily as a noxious chemical species, recent studies have established its significance as the third most essential gasotransmitter (after NO and CO)[6–8] which controls various physiological processes in nervous, respiratory, endocrine and immune systems.[6,7] It also dilates blood vessels and lowers blood pressure by acting as a smooth muscle reluctant and K-ATP channel opener. Furthermore, the effects of H_2S in gastrointestinal insulin signalling and as a regulator of energy production in mammalian cells under stress condition are also known.[9] In recent times, H_2S releasing prodrugs are used for treatments of cardiovascular, reperfusion injury and inflammatory diseases.[10,11] Overexpression of H_2S producing enzymes[12,13] is related to various diseases *e.g.* Alzheimer's disease,[14] Down's syndrome,[15] diabetes,[16] and liver cirrhosis.[17]

Because of the increasing interest in H_2S research, proper understanding of its production, mode of action and consumption is very essential. However, its optimal level in biological systems is debatable, as the concentration varies in the range over 10^5 orders.[18] Very short half-life of the species is a critical limitation for its accurate determination. Therefore, reliable and accurate determination methods for H_2S sensing in biological samples have appeared as burgeoning interests to acquire better knowledge of physiological and pathological functions. Several fluorescent probes were reported for *in vitro* as well as *in vivo* detection of the species. These probes were designed to accomplish rapid response, selectivity and sensitivity towards H_2S. These strategies include: (a) H_2S mediated reduction of azide to amine,[19–29] (b) H_2S trapping by nucleophilic addition,[30–34] (c) copper sulfide precipitation,[35–37] and (d) thiolysis of dinitrophenyl ether.[38] Among these, the azide reduction strategy has been extensively applied in numerous fluorescent probes. H_2S (pK_a = 6.9) is a better nucleophile[32] compared to other biothiols such as Cysteine (Cys, pK_a = 8.4) and glutathione (GSH, pK_a = 9.7).[39] Moreover, H_2S also exhibits dual nucleophilic character which discriminates it from other biothiols.[40] These features of H_2S were helpful in the design of various cascade reaction based probes. In 2011, Xian and co-workers reported fluorescence off–on probes based on cascade reaction demonstrating the selective and sensitive detection of H_2S.[33,34]

The first strategy incorporating H_2S mediated azide-to-amine reduction, in cascade reaction model was reported by Han *et al.*[41] Based on their design, the probe **1** (Fig. 1A) upon reduction of

Department of Chemistry, Indian Institute of Science Education and Research, Pune, India. E-mail: ptalukdar@iiserpune.ac.in; Fax: +91 20 2590 8186; Tel: +91 20 2590 8098

† Electronic supplementary information (ESI) available: Additional experimental procedures, fluorescence spectra. See DOI: 10.1039/c4ra13086c

the azide group facilitated an intramolecular cyclization to release a fluorescent coumarin derivative (Fig. 1B, route a). However, use of organic co-solvent (acetonitrile 20% v/v), long response time (20–40 min), low sensitivity, high detection limit (100 μM) and blue emission of the coumarin fluorophore limits its further biological applications. Guo and co-workers reported an alternate cascade reaction based probe **2** (Fig. 1A) which works *via* nucleophilic substitution of iodide by H_2S, leading to a cyclization and release of fluorescein (Fig. 1B, route b). This strategy partially addressed the limitation related to blue-shifted emission in the probe **1**.[42] Although, the probe **2** displayed a faster response time (5 min) and a lower detection limit (0.1 μM) compared to **1**, the sensitivity of the probe was not significant (50-fold) compared to other existing probes. The use of high concentration of a surfactant (20 mM cetrimonium bromide [CTAB]) in sensing studies limits its applicability in biological systems.[43]

The use of dissimilar fluorophores in these probes also impedes the comparison of two cascade reaction mechanisms because; physicochemical property of the probe is largely influenced by the nature of fluorophore. Therefore, introduction of an identical fluorophore was proposed to minimize structural differences and establish a better comparison between two aforementioned reaction mechanisms. Herein, we report design, synthesis and H_2S sensing abilities of two probes **Reso-N$_3$** and **Reso-Br** (Fig. 1A) to carry out a performance comparison of two cascade reaction models. Resorufin was selected as a fluorophore owing to its excellent chromogenic and fluorogenic properties.[44–51] Photophysical properties in the visible region, water solubility and excellent biocompatibility have already established the significance of resorufin in the development of fluorescence probes with *in vitro* and *in vivo* applications. Quenched fluorescence states for these probes was rationalized easily because, esterification of the hydroxyl group at C_7-position of resorufin is known to provide non-fluorescent species.[47]

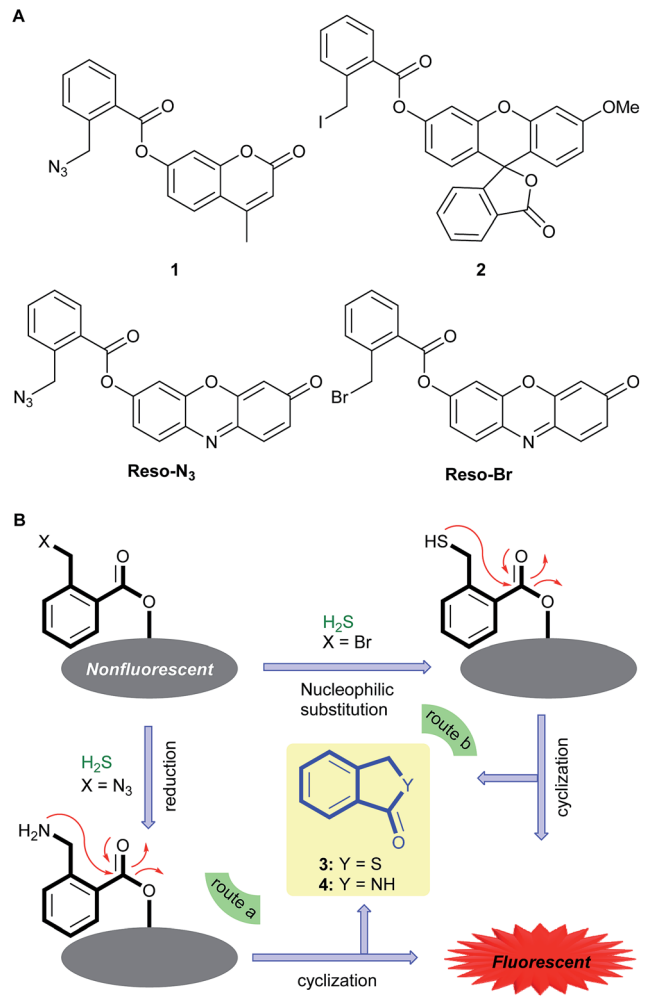

Fig. 1 Structures of the reported probes **1**–**2** and proposed probes **Reso-N$_3$** and **Reso-Br** (A). Cascade reaction based strategies for H_2S sensing (B).

Results and discussion

Addressing water solubility of Reso-N$_3$ and Reso-Br

To ensure the water solubility and cell membrane permeation of the designed probes, **Reso-N$_3$** and **Reso-Br**, respective *C* log *P* (the logarithm of the partition coefficient between water and 1-octanol) values were predicted using ChemBio-Draw 14.0 program and values were also compared with those of probes **1** and **2**. The program provided *C* log *P* = 4.54, 4.21, 4.93 and 6.48 for **Reso-N$_3$**, **Reso-Br**, **1** and **2**, respectively (Fig. S1†). Considering the Lipinski's rule of five,[52,53] the **Reso-N$_3$** and **Reso-Br** probes were expected to be more appropriate for sensing H_2S in the water and better cell permeable over probes **1** and **2**. The bromo leaving group in **Reso-Br** instead of an iodo was considered because the manipulation provides improved *C* log *P* value compared to the corresponding iodo derivative (Fig. S1†).

Synthesis of Reso-N$_3$ and Reso-Br

Synthesis of **Reso-N$_3$** and **Reso-Br** were carried out from acids **6** and **9**, respectively. Prior to the synthesis of **Reso-N$_3$**, ester **5** was converted to the acid **6** *via* the sequential benzylic bromination,

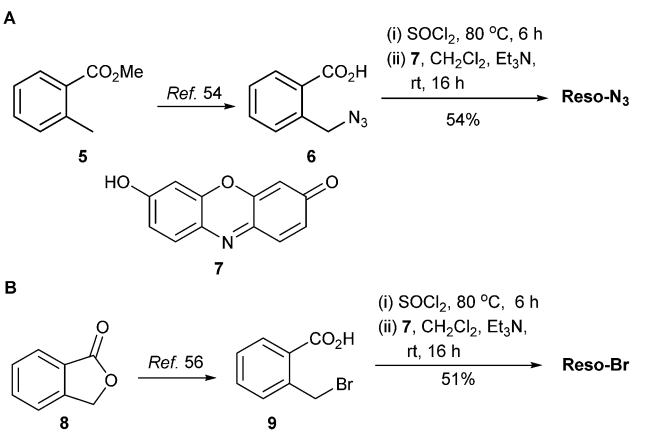

Scheme 1 Synthesis of **Reso-N$_3$** (A) and **Reso-Br** (B).

nucleophilic substitution of bromide by azide and ester hydrolysis.[54,55] Acid **6** was then converted to acid chloride which was further treated with **7** to furnish **Reso-N$_3$** (54%) as red solid. Pthalide **8** was first converted to acid **9** following a reported protocol.[56] Compound **9** was treated further with $SOCl_2$ followed by addition of resorufin **7** to obtain **Reso-Br** as red solid (51%) (Scheme 1).

Comparison of photophysical properties between Reso-N$_3$ and Reso-Br

After synthesizing **Reso-N$_3$** and **Reso-Br**, their background fluorescence properties were compared. Based on dynamic light scattering (DLS) studies, both probes (0–100 μM) were confirmed to be soluble in water. Therefore, photophysical properties and H_2S sensing properties of these probes were determined in water. UV-visible spectrum of **Reso-N$_3$** (10 μM) in water (Fig. 2A) exhibited weaker absorption signals at 318 nm ($\varepsilon = 2400\ M^{-1}\ cm^{-1}$), 344 nm ($\varepsilon = 2000\ M^{-1}\ cm^{-1}$) and 419 nm ($\varepsilon = 1100\ M^{-1}\ cm^{-1}$). On the other hand, **Reso-Br** (10 μM) exhibited absorption maxima at $\lambda_{max} = 364$ nm ($\varepsilon = 9000\ M^{-1}\ cm^{-1}$) and a less intense peak at 443 nm. When fluorescence intensities were monitored at $\lambda = 585$ nm ($\lambda_{ex} = 540$ nm), probe **Reso-N$_3$** displayed 0.17 times lower background fluorescence compared to probe **Reso-Br** (Fig. 2B). Therefore, **Reso-N$_3$** was expected to exhibit better off–on response during sensing of H_2S compared to **Reso-Br** because, both probes are identical fluorophore releasers.

Kinetics of H$_2$S sensing by Reso-N$_3$ and Reso-Br in water

In the next stage, response times of probes **Reso-N$_3$** (10 μM) and **Reso-Br** (10 μM) during H_2S sensing were determined under pseudo first order reaction conditions. Emission spectra ($\lambda_{ex} =$ 540 nm) were acquired at definite time intervals for each probe after addition of Na_2S (5 mM) and fluorescence intensities at 585 nm were plotted against time. For **Reso-N$_3$**, a pseudo first order reaction kinetics was observed with rate constant, $k = 0.6\ min^{-1}$ and half-life $t_{1/2} = 1.2$ min (Fig. 3A and S5A†). A similar kinetic profile was observed for **Reso-Br** with $k = 0.28\ min^{-1}$ and $t_{1/2} = 2.4$ min (Fig. 3B and S5B†). Sensing processes were completed within 6 min and 10 min for **Reso-N$_3$** and **Reso-Br**, respectively. These experiments confirm the faster response of the probe **Reso-N$_3$** compared to **Reso-Br** in water. Fluorescence kinetics experiments also suggest the stability and inertness of each probe, **Reso-N$_3$** and **Reso-Br** towards other biothiols (Fig. 3), Cys (5 mM) and GSH (5 mM).

Quantitative response of Reso-N$_3$ and Reso-Br towards H$_2$S in water

Responses of probes **Reso-N$_3$** (10 μM) and **Reso-Br** (10 μM) towards H_2S were evaluated by UV-visible spectroscopy. Na_2S (0–5 mM) was added into the solution of each probe (10 μM), and UV-visible spectra were recorded after 10 min of each addition. For **Reso-N$_3$** probe, the changes of 318, 344 and 419 nm bands were less prominent but, the formation of a 572 nm band indicated the formation resorufin **7** during the sensing process (Fig. 4A and S2†). For **Reso-Br**, sharp decrease in absorption bands 364 and 443 nm was observed (Fig. 4B). The sensing of H_2S by **Reso-Br** also resulted in the appearance of a strong band at 572 nm that corresponds to the formation of resorufin **7** (Fig. S2†).

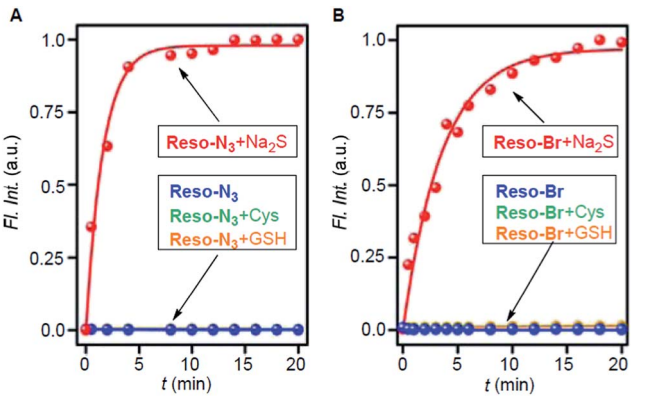

Fig. 3 Fluorescence kinetics of probes **Reso-N$_3$** (A) and **Reso-Br** (B) towards H_2S, Cys and GSH in water, recorded at 585 nm ($\lambda_{ex} =$ 540 nm).

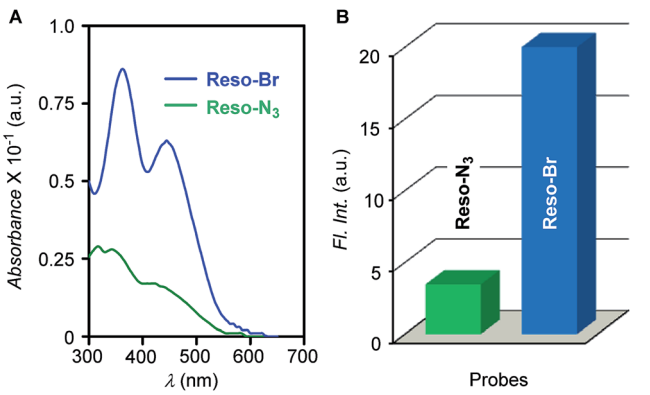

Fig. 2 UV-visible spectra of **Reso-N$_3$** and **Reso-Br** (10 μM each) in water (A); comparison of fluorescence intensity at 585 nm ($\lambda_{ex} = 540$ nm) of both probes (10 μM) in water (B).

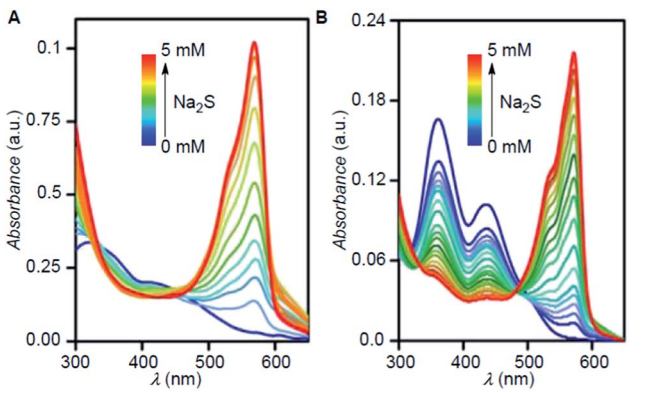

Fig. 4 UV-Visible titration spectra of **Reso-N$_3$** (A) and **Reso-Br** (B) with increasing concentration of Na_2S in water.

Next stage, fluorometric titrations were carried out to estimate quantitative responses of probes **Reso-N$_3$** (Fig. 5A) and **Reso-Br** (Fig. 5B) towards H_2S. Sharp enhancements in fluorescence intensities at 585 nm (λ_{ex} = 540 nm) were observed when increasing concentration of Na_2S (0 to 5 mM) was added to each probe in the water. **Reso-N$_3$** exhibited 614-fold fluorescence enhancement, which is significantly better than 414-fold jump determined for **Reso-Br** (Fig. S4†). The limit of detection (LOD) for H_2S sensing by **Reso-N$_3$** was 440 nM (Fig. S7A and Table S1†). The outcome was slightly better than the LOD = 550 nM calculated for **Reso-Br** (Fig. S7B and Table S2†).

Encouraged by fast response time and low LOD values of probes **Reso-N$_3$** and **Reso-Br**, water sample analyses were conducted to detect trace amounts of H_2S (or S^{2-}).[57] As expected, no H_2S was detected in the collected samples of tap water. When these water samples were spiked with a measured quantity of Na_2S, quantitative responses were observed for both **Reso-N$_3$** (Fig. 6A) and **Reso-Br** (Fig. 6B).

High sensitivity of probes **Reso-N$_3$** and **Reso-Br** during H_2S detection led us to evaluate their specificity to the analyte in an isolated and competitive environment with other biorelevant species. Each probe (10 μM) was treated with an analyte (NaF, NaCl, NaBr, NaI, Na_2SO_3, Na_2SO_4, $Na_2S_2O_3$, NaSCN, $NaNO_2$, $NaNO_3$, Cys, GSH and Hcy; 5 mM each), and fluorescence spectra were recorded after 10 min of addition. No significant fluorescence enhancements were observed in the case of any analyte (Fig. 7 and S8†). When Na_2S was added further to each of aforementioned solutions, the observed fluorescence enhancements were similar to that of only Na_2S addition. This data confirm the selectivity of each probe towards H_2S. Addition of a thiol containing amino acid (either of Cys, GSH and Hcy) to each probe did not show any significant increment of fluorescence. But, further addition of Na_2S to these solutions did not exhibit the expected fluorescence enhancement. These results were surprising considering the established selectivity of two cascade mechanisms towards H_2S. A plausible explanation of the unanticipated results can be attributed to the Michael addition of aliphatic thiols on resorufin leading to the formation of adducts that are nonfluorescent.[58]

The reduction-cyclization and nucleophilic substitution-cyclization mechanisms for detection of H_2S by **Reso-N$_3$** and **Reso-Br** were further studied by ^{1}H NMR titrations. Upon stepwise addition of Na_2S to the solutions of probes, decrease of peaks corresponds to **Reso-N$_3$** (Fig. S13†) and **Reso-Br** (Fig. S14†) with a simultaneous appearance of new peaks corresponding to resorufin 7 was observed in both the cases.

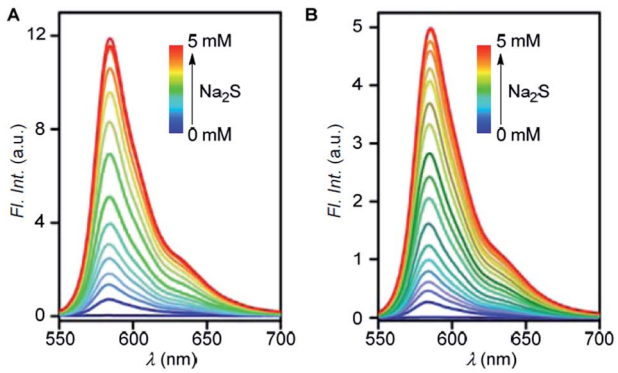

Fig. 5 Fluorescence titration spectra of **Reso-N$_3$** (A) and **Reso-Br** (B) with Na_2S in water. In each experiment, 10 μM of probe was treated with Na_2S (0–5 mM) and fluorescence spectrum (λ_{ex} = 540 nm) was recorded after 10 min of addition.

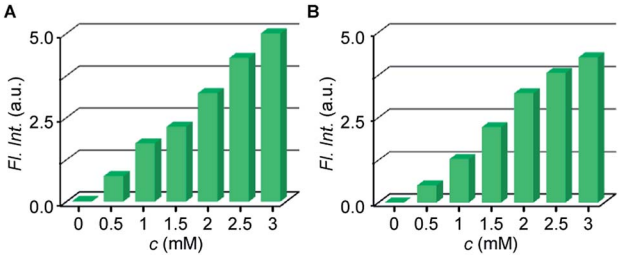

Fig. 6 Bar diagram, representing relative fluorescence intensity enhancements at 585 nm (λ_{ex} = 540 nm) for **Reso-N$_3$** (A) and **Reso-Br** (B) towards various tap water samples having different amount of Na_2S.

H_2S sensing properties of Reso-N$_3$ under physiological conditions

Further assessments of these two probes were carried out under physiological conditions. Probe **Reso-Br** was not stable in varied aqueous buffer (pH = 7.4) conditions and resulted in the rapid release of fluorophore 7 with the time (Fig. S9 and S10†). The instability of the **Reso-Br** probe can be corroborated to its solvolysis under the weakly nucleophilic media[59,60] followed by cyclization to release resorufin 7 (Scheme S1†). This outcome is not unanticipated for a benzyl bromide system with carboxylic

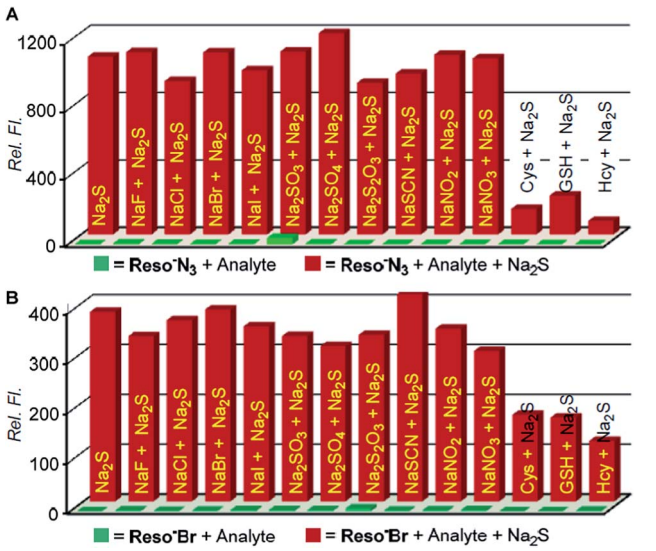

Fig. 7 Relative fluorescence intensity enhancements at 585 nm for, (A) **Reso-N$_3$** (10 μM) and (B) **Reso-Br** (10 μM) towards Na_2S (5 mM) in water. Front row: change in intensities in the presence of various analytes (5 mM); rear row: Na_2S was added in the presence of respective analyte.

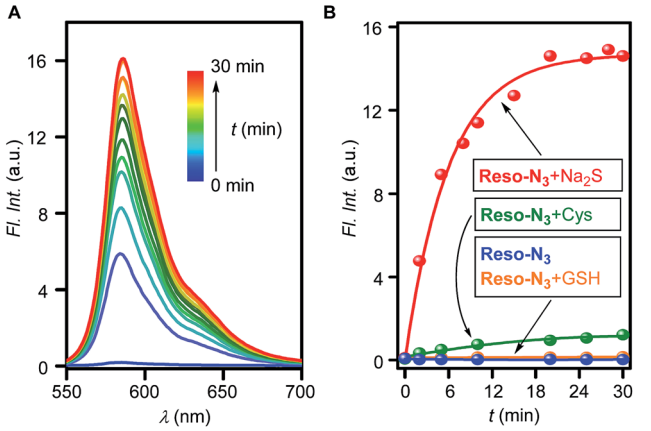

Fig. 8 Fluorescence spectra of **Reso-N$_3$** (10 μM) upon addition of Na_2S (5 mM) in phosphate buffer (5 mM, pH = 7.4) recorded with increasing time (A) and corresponding fluorescence kinetics diagram (B) generated by plotting intensity at $\lambda = 585$ nm ($\lambda_{ex} = 540$ nm) *versus* time. Stability of probe **Reso-N$_3$** in phosphate buffer (5 mM, pH = 7.4), in absence and in presence of Cys (5 mM), GSH (5 mM) are also presented.

ester moiety (an electron withdrawing group) at the *ortho*-position of aryl ring. **Reso-N$_3$** in contrast, was stable under aqueous buffer (pH = 7.4) conditions (Fig. 8B and S9†). The probe **Reso-N$_3$** (10 μM) upon reaction with Na_2S (5 mM) in phosphate buffer (5 mM, pH = 7.4) exhibited a pseudo first order reaction kinetics with rate constant, $k = 0.13$ min^{-1} and $t_{1/2} = 5.33$ min (Fig. S6†). The sensing process completes within 18 min after addition of H_2S (Fig. 8A). The fluorescence enhancement for **Reso-N$_3$** probe was limited to only H_2S and addition of either GSH or Cys provided no significant fluorescence enhancement (Fig. 8B).

The quantitative response of **Reso-N$_3$** towards H_2S was evaluated in buffer (5 mM, pH = 7.4) by UV-visible spectroscopy and fluorometric titrations. A gradual decrease in absorption maxima at 318 nm with sharp increment at 572 nm peak was observed with stepwise addition of Na_2S (Fig. 9A). When fluorometric titration was carried out for **Reso-N$_3$** in phosphate buffer (5 mM, pH = 7.4), addition of Na_2S results in a gradual increase in fluorescence intensity (Fig. 9B). When fluorescence intensity at 585 nm was plotted against the concentration of added Na_2S an excellent linear correlation ($R^2 = 0.98095$) was obtained (Fig. S11†). A detection limit of 4.15 μM was calculated based on signal to noise ratio, $S/N = 3$ (Table S3†).

Further, the selectivity of **Reso-N$_3$** towards H_2S over other analytes was evaluated under comparable conditions. When the probe was treated with ranges of analytes (NaF, NaCl, NaBr, NaI, Na_2SO_3, Na_2SO_4, $Na_2S_2O_3$, NaSCN, $NaNO_2$, $NaNO_3$, Ala, Ser, Cys, GSH or Hcy) in phosphate buffer (5 mM, pH = 7.4), no significant increment in fluorescence intensity was observed (Fig. 10A, front row). On the other hand, strong enhancement in fluorescence intensity was observed when Na_2S was added to the probe (Fig. 10A, the leftmost column of the rear row). Addition of Na_2S to solutions of the probe and competing analyte resulted in strong fluorescence intensity enhancements (Fig. 10A, rear row). The response of Na_2S towards the probe in the presence of Cys improved than that observed in pure water. Cuvette images taken under ambient light suggests a change in color from yellow to pink upon addition of only Na_2S to the probe **Reso-N$_3$** (Fig. 10B). Similarly, the appearance of orange fluorescent for the probe in the presence of Na_2S under the hand held UV-lamp ($\lambda_{ex} = 365$ nm) also corroborates to the selectivity of probe towards H_2S over other analytes (Fig. 10C).

Live cell imaging of intracellular H_2S by Reso-N$_3$

To evaluate the ability of **Reso-N$_3$** for detecting H_2S in the biological systems, live cell imaging studies were carried out using

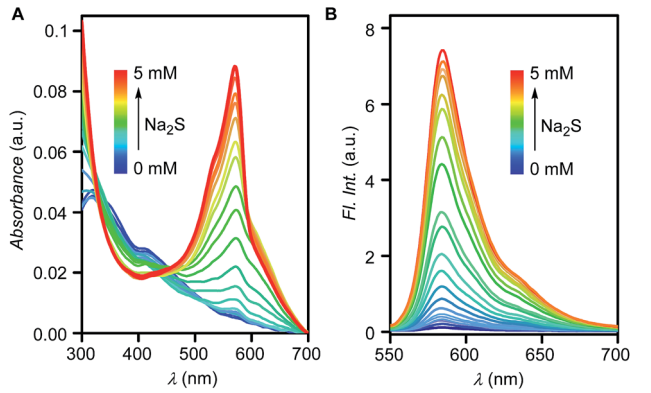

Fig. 9 UV-visible (A) and fluorescence spectra (B) of **Reso-N$_3$** (10 μM) with increasing concentration of Na_2S (0 to 5 mM) in phosphate buffer (5 mM, pH = 7.4).

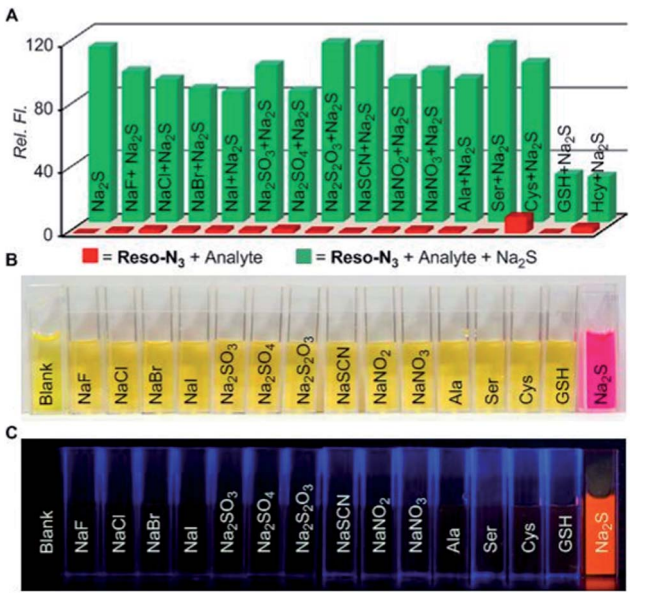

Fig. 10 Relative fluorescence intensity enhancements at 585 nm for **Reso-N$_3$** (10 μM) towards Na_2S (5 mM) and other analytes in phosphate buffer (A). Front row: change in intensities in the presence of various analytes (5 mM); rear row: Na_2S was added in the presence of respective analyte. Cuvette images of **Reso-N$_3$** (50 μM) in phosphate buffer (5 mM, pH = 7.4) in presence of various analytes taken under ambient light (B) and under hand held UV lamp, $\lambda_{ex} = 365$ nm (C).

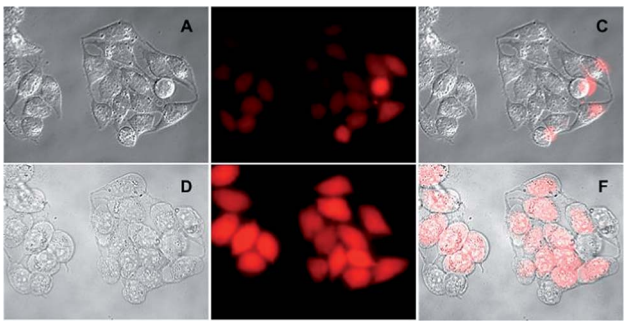

Fig. 11 Live cell imaging of HeLa cell: DIC (A), fluorescence (B) and overlay (C) images of cells, incubated with **Reso-N_3** (10 μM) for 15 min. (D–F) are respective DIC, fluorescence and overlay image of HeLa cells, preincubated with **Reso-N_3** (10 μM) followed by incubation with Na_2S (1 mM) for 15 min.

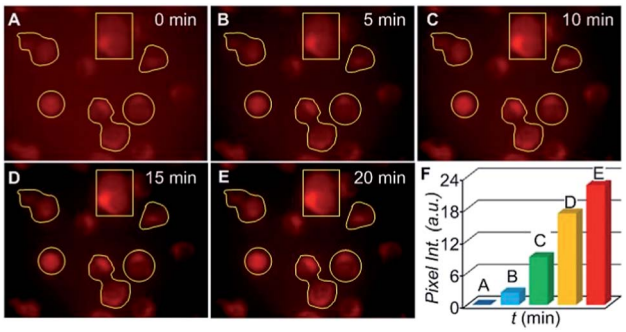

Fig. 12 Fluorescence images of HeLa cell acquired at different time intervals (0, 5, 10, 15 and 20 min) after incubating with Na_2S (A–E). Bar diagram was plotted by the average pixel intensity of selected ROI's *versus* time (F).

HeLa cells. When cells were incubated with only **Reso-N_3** (10 μM, in PBS buffer, pH = 7.4) for 15 min, very low fluorescence was observed. The weak fluorescence is attributed to the low levels of intracellular H_2S. Strong fluorescence was observed when cells, preincubated with probe, were incubated with Na_2S (1 mM, in PBS buffer, pH = 7.4) for 15 min (Fig. 11).

Finally, the quantitative response of probe **Reso-N_3** towards intracellular H_2S was studied. Quantification was done by recording the pixel intensity of the selected region of interest (ROI) from images acquired at different time intervals (0, 5, 10, 15, 20 min), after incubation with Na_2S. When pixel intensity values were plotted in a bar diagram against time, an increase in intensity was observed up to 20 min of incubation (Fig. 12). The gradual increment in intensity corresponds to an increase in intracellular H_2S concentration.

Conclusions

In summary, we have developed two fluorescent probes **Reso-N_3** and **Reso-Br** for sensing of H_2S under physiological conditions. **Reso-N_3** undergoes azide-to-amine reduction by H_2S followed by cyclization to release resorufin fluorophore. On the other hand, **Reso-Br** probe facilitates nucleophilic substitution of bromide by H_2S followed by cyclization to release the same fluorophore. The *C* log *P* guideline based on Lipinski's rule of five was also considered in the design, to favour water solubility and cell membrane permeation of these molecules. **Reso-N_3** was prepared from methyl 2-methylbenzoate in three steps with overall 27% yield. **Reso-Br** probe was synthesized from pthalide in two steps with overall 25% yield. Photophysical properties of these probes in water provided a lower background fluorescence for **Reso-N_3** compared to **Reso-Br**. H_2S sensing by **Reso-N_3** under the pseudo first order reaction kinetics provided rate constant, $k = 0.6\ min^{-1}$ and $t_{1/2} = 1.2$ min. Response of the probe **Reso-Br** towards H_2S under similar conditions was significantly faster with $k = 0.28\ min^{-1}$ and half life $t_{1/2} = 2.4$ min. **Reso-N_3** displayed 614-fold off–on fluorescence with detection limit = 440 nM. For **Reso-Br**, considerably reduced sensitivity of 414-fold and detection limit = 580 nM were determined. ^1H NMR titration experiments were carried out to prove the sensing mechanisms for each probe. Moreover under physiological conditions (in aqueous buffer, pH = 7.4) **Reso-Br** was found to be unstable, possibly due to its solvolysis under the weakly nucleophilic media. **Reso-N_3** on the other hand was stable under the comparable conditions. During H_2S sensing under these conditions, the **Reso-N_3** probe displayed $k = 0.13\ min^{-1}$, $t_{1/2} = 5.33$ min and sensitivity of 110-fold. Live cell imaging studies demonstrated applicability of **Reso-N_3** in the detection of intracellular H_2S.

Experimental section

I. General methods

All reactions were conducted under a nitrogen atmosphere. All the chemicals were purchased from commercial sources and used as received unless stated otherwise. Solvents: petroleum ether and ethyl acetate (EtOAc) were distilled prior to thin layer and column chromatography. Dichloromethane (DCM) was pre-dried over calcium hydride and then distilled under vacuum. Column chromatography was performed on Merck silica gel (100–200 mesh). TLC was carried out with E. Merck silica gel 60-F254 plates.

II. Physical measurements

The ^1H and ^{13}C spectra were recorded on 400 MHz Jeol ECS-400 (or 100 MHz for 13C) spectrometers using either residual solvent signals as an internal reference or from internal tetramethylsilane on the δ scale ($CDCl_3$ δ_H, 7.24 ppm, δ_C 77.0 ppm). The chemical shifts (δ) were reported in ppm and coupling constants (J) in Hz. The following abbreviations were used: m (multiplet), s (singlet), br s (broad singlet), d (doublet), t (triplet) dd (doublet of doublet). High-resolution mass spectra were obtained from MicroMass ESI-TOF MS spectrometer. FT-IR spectra were obtained using NICOLET 6700 FT-IR spectrophotometer as KBr disc and reported in cm^{-1}. Melting points were measured using a VEEGO Melting point apparatus. All melting points were measured in open glass capillary and values are uncorrected. Absorption spectra were recorded on a PerkinElmer, Lambda 45 UV-Vis spectrophotometer. Steady State

fluorescence experiments were carried out in a micro fluorescence cuvette (Hellma, path length 1.0 cm) on a Fluoromax 4 instrument (Horiba Jobin Yvon). Cell images were taken in 35 mm (diameter) dishes. The media (DMEM) and PBS buffer were purchased from commercial sources. Fluorescence images were taken using Olympus Inverted IX81 equipped with Hamamatsu Orca R2 microscope. ChemBio Draw Ultra and Image J software were used for drawing structure and for processing cell image respectively.

III. Synthesis of probes Reso-N_3 and Reso-Br

Synthesis of methyl 2-(azidomethyl)benzoic acid 6 ($C_8H_7N_3O_2$)[54,55]

Step A. To the solution of 2-methylbenzoate **5** (1.00 g, 6.65 mmol) in dry CCl_4 (10 mL) were added *N*-bromosuccinimide (1.30 g, 7.32 mmol), and benzoyl peroxide (0.032 g, 0.133 mmol). The reaction mixture was stirred at 80 °C for 8 h. Subsequently, the reaction mixture was cooled to room temperature and placed in an ice-water bath to allow the precipitation of succinimide. The reaction mixture was diluted with dichloromethane (50 mL) and filtered. The filtrate was washed with saturated NH_4Cl (30 mL). The organic layer was dried over Na_2SO_4 and concentrated under reduced pressure to afford 2-(bromomethyl) benzoate as yellow oil. The crude product was used for the next reaction without further purification.

Step B. To the solution of 2-(bromomethyl)benzoate in DMF (10 mL) was added sodium azide (0.570 g, 8.72 mmol), and the reaction mixture was stirred at 70 °C for 16 h. At the completion of the reaction, the solution was cooled to room temperature. To the reaction mixture was added water (30 mL) and the product extracted with ethyl acetate (3 × 30 mL). The combined organic layer was washed with brine (40 mL), dried over Na_2SO_4, and concentrated under reduced pressure to obtain methyl 2-(azidomethyl)benzoate (0.665 g) as yellow oil. The crude product was used for the next reaction without further purification.

Step C. In a 50 mL round bottomed flask, was placed methyl 2-(azidomethyl)benzoate and 20 mL of 2 N NaOH/MeOH (1 : 1) was added. After 1 h stirring at room temperature the reaction mixture was acidified with 1 N HCl (upto pH = 1) and product was extracted with of chloroform (3 × 30 mL). The combined organic layer was dried over Na_2SO_4 and concentrated under reduced pressure to afford 2-(azidomethyl)benzoic acid **6** (0.67 g, 52%) as white solid. ^{1}H NMR (400 MHz, CD_3OD): δ 8.03 (d, J = 7.8 Hz, 1H), 7.56 (dd, J = 11.8, 4.3 Hz, 1H), 7.52–7.38 (m, 2H), 4.79 (s, 2H). ^{13}C NMR (100 MHz, CD_3OD): δ 169.92, 138.47, 133.59, 132.33, 131.33, 131.01, 129.27, 53.91.

Synthesis of 3-oxo-3*H*-phenoxazin-7-yl 2-(azidomethyl) benzoate, Reso-N_3 ($C_{20}H_{12}N_4O_4$). In a oven dried 25 mL round bottomed flask were added 2-(azidomethyl)benzoic acid **6** (100 mg, 0.29 mmol) and $SOCl_2$. The reaction mixture was refluxed under inert atmosphere for 6 h. The reaction mixture was cooled to room temperature and concentrated under reduced pressure to obtain crude 2-(azidomethyl)benzoic acid chloride as yellowish oil. The crude oil was added dropwise to the suspension of resorufin **7** (100 mg, 0.425 mmol) in dry dichloromethane (5 mL) and the reaction mixture was stirred at room temperature for 16 h. At completion, the reaction mixture was dried under reduce pressure and then subjected to column chromatography over silica gel (eluent: 18% EtOAc in petroleum ether) to obtain pure **Reso-N_3** (76 mg, 54%) as dark red solid. M.p.: 168–169 °C (decomposed); IR (KBr): ν_{max} cm^{-1} 3450, 3045, 2103, 1739, 1614, 1509, 1438, 1242, 1033, 862; ^{1}H NMR (400 MHz, $CDCl_3$): δ 8.28 (dd, J = 7.8, 1.3 Hz, 1H), 7.87 (d, J = 8.6 Hz, 1H), 7.70 (td, J = 7.6, 1.3 Hz, 1H), 7.61 (d, J = 6.9 Hz, 1H), 7.57–7.49 (m, 1H), 7.46 (d, J = 9.9 Hz, 1H), 7.31–7.21 (m, 3H), 6.88 (dd, J = 9.8, 2.0 Hz, 1H), 6.35 (s, 1H), 4.88 (s, 2H). ^{13}C NMR (100 MHz, $CDCl_3$): δ 186.78, 164.64, 153.87, 149.72, 148.88, 144.87, 139.07, 135.67, 135.27, 134.54, 132.26, 131.86, 131.72, 130.66, 128.94, 127.34, 119.89, 110.40, 107.74, 77.80, 77.48, 77.16, 53.56. HRMS (ESI): calc. for $C_{20}H_{12}N_4O_4Na^+$: 395.0756 $[M + Na]^+$; found: 395.0757.

Synthesis of 2-(bromomethyl) benzoic acid 9 ($C_8H_7BrO_2$).[56] To a 25 mL round bottom flask was added pthalide **8** (500 mg, 3.37 mmol) and dissolved in glacial acetic acid (5 mL). To the resulting solution was added drop wise a solution of 33% HBr-AcOH (10 mL) and stirred at room temperature for 2 h. Subsequently, the reaction mixture was heated at 70 °C for 1.5 h followed by stirring at room temperature for overnight. The reaction mixture was then poured into ice-water (100 mL) and the resulting white precipitate was filtered. The residue was washed with ice-water and dried under reduced pressure to obtain compound **9** (400 mg, 50%) as white solid. The crude product was used for the next reaction without further purification. M.p. 157–158 °C; ^{1}H NMR (400 MHz, CD_3OD): δ 7.96 (d, J = 7.4 Hz, 1H), 7.55–7.45 (m, 2H), 7.44–7.34 (m, 1H), 5.02 (s, 2H). ^{13}C NMR (100 MHz, CD_3OD): δ 169.57, 140.66, 133.24, 132.60, 132.20, 129.31, 49.00, 31.75.

Synthesis of 3-oxo-3*H*-phenoxazin-7-yl 2-(bromomethyl) benzoate, Reso-Br ($C_{20}H_{12}BrNO_4$). In a oven dried 25 mL round bottomed flask were added 2-(bromomethyl)benzoic acid **9** (100 mg, 0.29 mmol) and $SOCl_2$. The reaction mixture was refluxed under inert atmosphere for 6 h. The reaction mixture was cooled to room temperature and concentrated under reduced pressure to obtain crude 2-(bromomethyl)benzoic acid chloride as yellowish oil. The crude oil was added dropwise to the suspension of resorufin **7** (100 mg, 0.425 mmol) in dry dichloromethane (5 mL) and the reaction mixture was stirred at room temperature for 16 h. At completion, the reaction mixture was dried under reduce pressure and then subjected to column chromatography over silica gel (Eluent: 18% EtOAc in petroleum ether) to obtain pure **Reso-Br** (80 mg, 51%) as dark red solid. M.p.: 180–181 °C (decomposed); IR (KBr): ν_{max} cm^{-1} 3432, 3043, 1730, 1630, 1558, 1312, 1241, 1120, 1027, 870. ^{1}H NMR (400 MHz, $CDCl_3$): δ 8.21 (dd, J = 7.8, 1.3 Hz, 1H), 7.87 (d, J = 8.5 Hz, 1H), 7.63 (td, J = 7.5, 1.4 Hz, 1H), 7.57–7.48 (m, 2H), 7.46 (d, J = 9.7 Hz, 1H), 7.35–7.28 (m, 2H), 6.88 (dd, J = 9.8, 2.0 Hz, 1H), 6.36 (d, J = 1.9 Hz, 1H); ^{13}C NMR (100 MHz, $CDCl_3$): δ 186.7, 164.5, 149.7, 148.7, 144.8, 140.7, 140.3, 135.6, 135.3, 134.3, 132.4, 132.2, 131.7, 129.2, 127.8, 119.9, 110.4, 107.7, 31.64. HRMS (ESI): calc. for $C_{20}H_{12}BrNO_4H^+$: 410.0028 $[M + H]^+$; found: 410.0052.

Acknowledgements

We acknowledge IISER Pune and DST-SERB (Grant no. SR/S1/OC-65/2012) for financial supports. T.S. thanks University Grant Commission (UGC) and D.K. thanks Council for Scientific and Industrial Research (CSIR) for research fellowships.

Notes and references

1 C. L. Evans, *Q. J. Exp. Physiol.*, 1967, **52**, 231–248.
2 T. L. Guidotti, *Int. J. Toxicol.*, 2010, **29**, 569–581.
3 S. Singh, D. Padovani, A. Leslie Rachel, T. Chiku and R. Banerjee, *J. Biol. Chem.*, 2009, **284**, 22457–22466.
4 D. Boehning and S. H. Snyder, *Annu. Rev. Neurosci.*, 2003, **26**, 105–131.
5 N. Shibuya, M. Tanaka, M. Yoshida, Y. Ogasawara, T. Togawa, K. Ishii and H. Kimura, *Antioxid. Redox Signaling*, 2009, **11**, 703–714.
6 L. Li, P. Rose and P. K. Moore, *Annu. Rev. Pharmacol. Toxicol.*, 2011, **51**, 169–187.
7 H. Kimura, *Amino Acids*, 2011, **41**, 113–121.
8 O. Kabil and R. Banerjee, *J. Biol. Chem.*, 2010, **285**, 21903–21907.
9 M. Fu, W. Zhang, L. Wu, G. Yang, H. Li and R. Wang, *Proc. Natl. Acad. Sci. U. S. A.*, 2012, **109**, 2943–2948.
10 A. Martelli, L. Testai, C. Breschi Maria, C. Blandizzi, A. Virdis, S. Taddei and V. Calderone, *Med. Res. Rev.*, 2012, **32**, 1093–1130.
11 J. L. Wallace, *Trends Pharmacol. Sci.*, 2007, **28**, 501–505.
12 K. Wang, S. Ahmad, M. Cai, J. Rennie, T. Fujisawa, F. Crispi, J. Baily, M. R. Miller, M. Cudmore, P. W. F. Hadoke, R. Wang, E. Gratacos, I. A. Buhimschi, C. S. Buhimschi and A. Ahmed, *Circulation*, 2013, **127**, 2514–2522.
13 C. Szabo, C. Coletta, C. Chao, K. Modis, B. Szczesny, A. Papapetropoulos and M. R. Hellmich, *Proc. Natl. Acad. Sci. U. S. A.*, 2013, **110**, 12474–12479.
14 K. Eto, T. Asada, K. Arima, T. Makifuchi and H. Kimura, *Biochem. Biophys. Res. Commun.*, 2002, **293**, 1485–1488.
15 P. Kamoun, M.-C. Belardinelli, A. Chabli, K. Lallouchi and B. Chadefaux-Vekemans, *Am. J. Med. Genet., Part A*, 2003, **116**, 310–311.
16 W. Yang, G. Yang, X. Jia, L. Wu and R. Wang, *J. Physiol.*, 2005, **569**, 519–531.
17 S. Fiorucci, E. Antonelli, A. Mencarelli, S. Orlandi, B. Renga, G. Rizzo, E. Distrutti, V. Shah and A. Morelli, *Hepatology*, 2005, **42**, 539–548.
18 K. R. Olson, *Biochim. Biophys. Acta*, 2009, **1787**, 856–863.
19 H. Peng, Y. Cheng, C. Dai, A. L. King, B. L. Predmore, D. J. Lefer and B. Wang, *Angew. Chem., Int. Ed.*, 2011, **50**, 9672–9675.
20 A. R. Lippert, E. J. New and C. J. Chang, *J. Am. Chem. Soc.*, 2011, **133**, 10078–10080.
21 L. A. Montoya and M. D. Pluth, *Chem. Commun.*, 2012, **48**, 4767–4769.
22 B. Chen, W. Li, C. Lv, M. Zhao, H. Jin, H. Jin, J. Du, L. Zhang and X. Tang, *Analyst*, 2013, **138**, 946–951.
23 G. Zhou, H. Wang, Y. Ma and X. Chen, *Tetrahedron*, 2013, **69**, 867–870.
24 S. K. Das, C. S. Lim, S. Y. Yang, J. H. Han and B. R. Cho, *Chem. Commun.*, 2012, **48**, 8395–8397.
25 M.-Y. Wu, K. Li, J.-T. Hou, Z. Huang and X.-Q. Yu, *Org. Biomol. Chem.*, 2012, **10**, 8342–8347.
26 Q. Wan, Y. Song, Z. Li, X. Gao and H. Ma, *Chem. Commun.*, 2013, **49**, 502–504.
27 R. Wang, F. Yu, L. Chen, H. Chen, L. Wang and W. Zhang, *Chem. Commun.*, 2012, **48**, 11757–11759.
28 F. Yu, P. Li, P. Song, B. Wang, J. Zhao and K. Han, *Chem. Commun.*, 2012, **48**, 2852–2854.
29 T. Saha, D. Kand and P. Talukdar, *Org. Biomol. Chem.*, 2013, **11**, 8166–8170.
30 Z. Xu, L. Xu, J. Zhou, Y. Xu, W. Zhu and X. Qian, *Chem. Commun.*, 2012, **48**, 10871–10873.
31 Y. Qian, L. Zhang, S. Ding, X. Deng, C. He, X. E. Zheng, H.-L. Zhu and J. Zhao, *Chem. Sci.*, 2012, **3**, 2920–2923.
32 Y. Qian, J. Karpus, O. Kabil, S.-Y. Zhang, H.-L. Zhu, R. Banerjee, J. Zhao and C. He, *Nat. Commun.*, 2011, **2**, 495.
33 C. Liu, J. Pan, S. Li, Y. Zhao, L. Y. Wu, C. E. Berkman, A. R. Whorton and M. Xian, *Angew. Chem., Int. Ed.*, 2011, **50**, 10327–10329.
34 C. Liu, B. Peng, S. Li, C.-M. Park, A. R. Whorton and M. Xian, *Org. Lett.*, 2012, **14**, 2184–2187.
35 K. Sasakura, K. Hanaoka, N. Shibuya, Y. Mikami, Y. Kimura, T. Komatsu, T. Ueno, T. Terai, H. Kimura and T. Nagano, *J. Am. Chem. Soc.*, 2011, **133**, 18003–18005.
36 F. Hou, L. Huang, P. Xi, J. Cheng, X. Zhao, G. Xie, Y. Shi, F. Cheng, X. Yao, D. Bai and Z. Zeng, *Inorg. Chem.*, 2012, **51**, 2454–2460.
37 F. Hou, J. Cheng, P. Xi, F. Chen, L. Huang, G. Xie, Y. Shi, H. Liu, D. Bai and Z. Zeng, *Dalton Trans.*, 2012, **41**, 5799–5804.
38 X. Cao, W. Lin, K. Zheng and L. He, *Chem. Commun.*, 2012, **48**, 10529–10531.
39 *Data for Biochemical Research*, ed. Dawson R. M. C., Oxford University Press, New York, NY, 3rd edn, 1987, pp. 16–17.
40 X. Wang, J. Sun, W. Zhang, X. Ma, J. Lv and B. Tang, *Chem. Sci.*, 2013, **4**, 2551–2556.
41 Z. Wu, Z. Li, L. Yang, J. Han and S. Han, *Chem. Commun.*, 2012, **48**, 10120–10122.
42 J. Zhang, Y.-Q. Sun, J. Liu, Y. Shi and W. Guo, *Chem. Commun.*, 2013, **49**, 11305–11307.
43 S.-H. Park and H.-K. Choi, *Int. J. Pharm.*, 2006, **321**, 35–41.
44 M. Sun, D. Shangguan, H. Ma, L. Nie, X. Li, S. Xiong, G. Liu and W. Thiemann, *Biopolymers*, 2003, **72**, 413–420.
45 S. Y. Kim and J.-I. Hong, *Org. Lett.*, 2007, **9**, 3109–3112.
46 M. G. Choi, S. Cha, J. E. Park, H. Lee, H. L. Jeon and S.-K. Chang, *Org. Lett.*, 2010, **12**, 1468–1471.
47 M.-G. Choi, J.-Y. Hwang, S.-Y. Eor and S.-K. Chang, *Org. Lett.*, 2010, **12**, 5624–5627.
48 W. Chen, Z. Li, W. Shi and H. Ma, *Chem. Commun.*, 2012, **48**, 2809–2811.
49 H. G. Im, H. Y. Kim, M. G. Choi and S.-K. Chang, *Org. Biomol. Chem.*, 2013, **11**, 2966–2971.

50 K. Cui, Z. Chen, Z. Wang, G. Zhang and D. Zhang, *Analyst*, 2011, **136**, 191–195.
51 W. Gao, B. Xing, R. Y. Tsien and J. Rao, *J. Am. Chem. Soc.*, 2003, **125**, 11146–11147.
52 C. A. Lipinski, F. Lombardo, B. W. Dominy and P. J. Feeney, *Adv. Drug Delivery Rev.*, 1997, **23**, 3–25.
53 P. Leeson, *Nature*, 2012, **481**, 455–456.
54 J. M. Smith, F. Vitali, S. A. Archer and R. Fasan, *Angew. Chem., Int. Ed.*, 2011, **50**, 5075–5080.
55 T. Wada, A. Ohkubo, A. Mochizuki and M. Sekine, *Tetrahedron Lett.*, 2001, **42**, 1069–1072.
56 J. McNulty and K. Keskar, *Org. Biomol. Chem.*, 2013, **11**, 2404–2407.
57 W. Sun, S. Nesic, D. Young and R. C. Woollam, *Ind. Eng. Chem. Res.*, 2008, **47**, 1738–1742.
58 Y. Shiraishi, K. Yamamoto, S. Sumiya and T. Hirai, *Chem. Commun.*, 2013, **49**, 11680–11682.
59 M. D. Bentley and M. J. S. Dewar, *J. Am. Chem. Soc.*, 1970, **92**, 3991–3996.
60 K.-T. Liu, Y.-F. Duann and S.-J. Hou, *J. Chem. Soc., Perkin Trans. 2*, 1998, 2181–2186.